Electronic Supplementary Material (ESI) for CrystEngComm.

Electronic supplementary information for

An innovative approach to resolution: using the nature of the achiral solvent to orient chiral resolution

Joséphine de Meester, Oleksii Shemchuk, Laurent Collard, Johan Wouters, Simon Baillieux, Koen Robeyns, Tom Leyssens*

*Corresponding author: tom.leyssens@uclouvain.be

Table of Contents

Experimental Procedures

1) Materials

(S)-1,1'-bi-2-naphtol (Merck), (R)-1,1'-bi-2-naphtol (Fluorochem), (rac)-1,1'-bi-2-naphtol (Acros Organics), (1R, 2R)-N,N′-Dimethyl-1,2-diphenylethane-1,2-diamine, toluene (VWR chemicals) and benzene (TCI) were purchased from commercial sources and used without further purification.
For convenience, 1,1'-bi-2-naphtol will be abbreviated as Binol, and N,N′-Dimethyl-1,2-diphenylethane-1,2-diamine as DADPE in the rest of the document.

2) Slurries

Slurry experiments were performed preparing equimolar suspensions (0.2mmol) of (S)- or (R)-Binol with (R,R)-DADPE at 20°C in methanol (MeOH) (0.2mL), ethanol (EtOH) (1mL), ethyl acetate (EtOAc) (0.5mL), dichloromethane (DCM) (0.2mL), toluene (1mL), isopropyl alcohol (IPA) (1mL) and benzene (1mL). The suspensions were stirred in a Cooling thermomixer HLC at 500 rpm. After 1 day of stirring, the vials were seeded with all possible solid forms, then let to equilibrate for 7 days. The suspensions were then filtered, the powders washed, dried and analyzed using PXRD.
Slurries of (S)-Binol with (R,R)-DADPE in the different solvents showed the same diffraction pattern as the reported cocrystal (S)-(R,R) (CCDC ref code **DICVUH**)[1]. Slurries of (R)Binol with (R,R)-DADPE in all solvents except benzene showed the same diffraction pattern as the cocrystal (R)-(R,R). Slurry of (R)-Binol with (R,R)-DADPE in benzene showed the same diffraction pattern as the cocrystal-solvate (R)-(R,R)-benzene.

3) Single crystal formation

3.1 (R)-(R,R) cocrystal

Single crystals of the (R)-(R,R) cocrystal were obtained by slow evaporation from toluene, starting from an undersaturated equimolar solution of (R)-Binol and (R,R)-DADPE. The solution was left to evaporate slowly at RT. Once crystals formed, a suitable crystal was retrieved and analyzed by SC-XRD.

3.2 (R)-(R,R)-benzene cocrystal solvate

Single crystals of the (R)-(R,R)-benzene cocrystal-solvate were obtained by slow evaporation from benzene, starting from an undersaturated equimolar solution of (R)-Binol and (R,R)-DADPE. The solution was left to evaporate slowly at RT. Once crystals formed, a suitable crystal was retrieved and analyzed by SC-XRD.

4) Solubility determination

The solubility curves were determined using a Crystal16 - Technobis Crystallization System. Different masses of (S)-(R,R) or (R)-(R,R) were weighed in vials, to which were added a magnetic stirrer and 0.8 mL of solvent. The following temperature profile was then applied:

- From 20°C to 0°C at -0.5°C/min,
- Hold at 0°C for 2 hours,
- Heat to *"desired temperature"* at 0.05°C/min,
- Hold at *"desired temperature"* for 2 hours,
- Cool to 0°C at 0.2°C/min.

For determining the (R)-(R,R)-benzene solubility curve, the (R)-(R,R) cocrystal was weighed and benzene was added. The mixtures were then let to equilibrate for 48 hours at 20°C under stirring before being placed in the Crystal16.

5) Ternary phase Diagrams

Slurries of (rac)-Binol with (R,R)-DADPE in benzene or toluene were made, seeded after 1 day with all possible solid forms, then stirred for 4 more days at 20°C. After that, the mixtures were filtered and the powders were analyzed by PXRD to determine the solid phase obtained in suspension. When needed, supplementary experiments (NMR and *c*HPLC) were made on the powder to determine the exact nature of the phases.

6) Upscaled resolutions of Binol

6.1 In toluene

(rac)-Binol (2g, 6.9852mmol) and (R,R)-DADPE (2.96140g, 13.9498mmol) were suspended in toluene (71mL) in a round bottom flask (100mL) with a stirring bar. The suspension was seeded with all possible solid forms, then stirred at 20°C at 500rpm for 5 days. The mixture was then filtered and the powder was washed with toluene. The powder (0.60013g) was analyzed by PXRD and *c*HPLC.

6.2 In benzene

(rac)-Binol (2g, 6.9852mmol) and (R,R)-DADPE (1.93599g, 9.1195mmol) were suspended in benzene (46mL) in a round bottom flask (100mL) with a stirring bar. The suspension was seeded with all possible solid forms, then stirred at 20°C at 500rpm for 4 days. The mixture was then filtered and the powder was washed with benzene. The powder (0.96503g) was analyzed by PXRD and *c*HPLC.

7) Powder X-ray diffraction (PXRD)

PXRD data were collected using a Siemens D5000 diffractometer equipped with a Cu X-ray source operating at 40 kV and 40 mA. A secondary monochromator was used to select the Kα radiation of Cu (λ = 1.5418 Å). A scanning range of 2θ values was applied from 5° to 35°.

8) Single crystal X-ray diffraction (SC-XRD)

SC-XRD data were collected using a MAR345 image plate detector with Mo Kα radiation (λ = 0.71073 Å), generated by an Incoatec IμS microfocus source. The collected data was integrated and reduced using CrystAlis^{PRO}[2] and the implemented absorption correction was applied. Structure solution was achieved using the dual-space algorithm in SHELXT[3] and the structure was further refined against F^2 by SHELXL[4]. All non-hydrogen atoms were refined anisotropically. Symmetry analysis and validation were carried out using PLATON[5]. Figures were generated using the molecular visualization software Mercury 2022.3.0[6].
(R)-(R,R) was crystallized using enantiopure starting materials and measured at room temperature. One phenyl ring was found disordered and refined in two parts to a ratio of 58/42. Similarity restrains are set up between both disordered rings as well as isotropic and rigid bond restraints on the thermal ellipsoids of the disordered parts. Chirality could be attributed as used starting materials were enantiopure.
For (R)-(R,R)-benzene crystals were transferred to Paratone® N oil to prevent evaporation of benzene. A single crystal was picked up on a nylon loop and quickly flash-frozen in a N_2 gas stream at 150K as tests at room temperature gave only poor diffraction ~2Å. Despite the low-temperature measurement only limited diffraction was observed and ultimately the diffraction limit was set to 1.1Å during integration, beyond which only poor diffraction was observed.
Both (R)-Binol and (R,R)-DADPE are found on a 2-fold crystallographic axis. The benzene molecule that is located inside the pocket surrounded by aromatic rings (Figure 2, in blue) is found close to a 2-fold axis and its occupancy was consequently constraint at 50% (the benzene molecule thus occupies a solvent pocket that is larger than the molecule itself and only loosely interacts with its surroundings). The second benzene molecule that is found in the solvent channel (Figure 2, in green) only partially occupies the site and its occupancy was refined to 87%. Possibly the solvent channel contains additional benzene molecules while still in solution (see TGA analysis) but these evaporate the moment the crystal is harvested from the crystallization solution as well as some of the benzene molecules that were located in the solvent channel (Figure 2, in green) hence the lower occupancy observed.
The solvent channels with disordered solvent were treated by the SQUEEZE procedure (PLATON[7]) to account for the diffuse electron density (a total of 102 electros were located in the solvent accessible volume of 597 Å^3).
Both the (R)-Binol and (R,R)-DADPE molecules show disorder. (R)-Binol is completely disordered, for DADPE the phenyl rings are found disordered. Both were refined in 2 parts (72/28) for (R)-Binol, (63/27) for the phenyl rings of (R,R)-DADPE. Both disordered parts were refined to be geometrically similar. For the minor disordered part of the (R)-Binol the thermal ellipsoid were constraint to be identical to the major part. Overall mild isotropic and rigid bond restraints were applied to all carbon atoms and more stringent ones to the disordered parts of (R,R)-DADPE. The NH_2 group of (R,R)-DADPE was restraint as an non planar group with geometric restraints on the geometry of the NH_2 group and the CNH angle, but no rotational restraints/constraints were set up for this NH_2 group.
See point 2 in the Results and Discussion here below for the crystallographic data and refinement details for both reported structures.

9) Thermal analyses

9.1 Thermogravimetric analyses (TGA)

TGA analyses were conducted using a Mettler Toledo TGA/DSC 3^+ instrument, varying the temperature from 25 to 600°C, with a heating rate of 10°C/min, under nitrogen with a flow rate of 50mL/min. Solid samples (5-10 mg) were placed in alumina pans.

9.2 Differential scanning calorimetry analyses (DSC)

DSC analyses were conducted using a TA Instrument DSC2500. The temperature range employed for (R)-(R,R) and (S)-(R,R) was from 20°C to 170°C, and for (R)-(R,R)-benzene from 20°C to 150°C, at a heating rate of 5°C/min under nitrogen with a flow rate of 50mL/min. Solid samples (5-10 mg) were placed in aluminum pans with perforated lid.

9.3 Variable temperature Powder X-ray diffraction analysis (VT-PXRD)

VT-PXRD was conducted using a glass capillary (0.7 mm diameter, Hilgenberg GmbH) filled with (R)-(R,R)-benzene. Prior to analysis, the capillary was cut and placed into molten wax on a goniometric head. The analysis was performed using a MAR345 image plate detector using MoKα radiation originating from an Incoatec Source^{HIGHBRILLIANCE} (IμS^{HIGHBRILLIANCE}) operating at 50 kV and 1000 μA (parallel beam, ELM47 mirror). X-ray exposures was carried out for 10 min (at 30°C, 60°C, 65°C and 70°C) and 5 min (at 35°C, 40°C, 45°C, 50°C and 55°C), during which the capillary with the sample was rotated by 180°. Diffraction data was integrated using Fit2D software (using data from a 0.1 mm diameter capillary filled with LaB_6 as calibrant). Heating the sample-containing capillary was performed with a Leister CH-6060 Sarnen hot air blower (Leister Technologies Benelux B.V.). The air blower was calibrated before the measure by a thermocouple housed in a capillary.

10) Chiral High-Performance Liquid Chromatography (cHPLC)

The separation of (R)- and (S)-Binol was performed by Chiral HPLC using a Waters Arc HPLC coupled with a 2998 PDA detector. Both enantiomers of Binol were separated on a Daicel Chiralpak IA column 250x4.6mm 5μm with a mix of 90% v/v isohexane, 10% v/v Isopropanol as mobile phase. The separation was performed at 25°C with a flow rate of 1mL/min.

11) Nuclear magnetic resonance (NMR)

^{1}H NMR spectra were measured on a 300MHz spectrometer Bruker. Chemical shifts are reported in parts per million (ppm) and were referenced regarding the chemical shift of the peak of the deuterated solvent used ($(CD_3)_2SO$ at 2.50ppm). Spectral multiplicities are described as follows: singlet (s), doublet (d), triplet (t), quartet (q), and multiplet (m).

Results and Discussion

1) Nuclear magnetic resonance (NMR)

Binol = ^{1}H NMR (300 MHz, DMSO) δ 9.20 (s, 1H), 7.86 (dd, *J* = 5.2, 3.9 Hz, 2H), 7.31 (d, *J* = 8.9 Hz, 1H), 7.26 – 7.12 (m, 2H), 6.93 (d, *J* = 8.2 Hz, 1H).
DADPE = ^{1}H NMR (300 MHz, DMSO) δ 7.23 – 7.02 (m, 1H), 3.81 (s, 1H), 1.94 (s, 1H).

2) Crystallographic data

2.1 Data

Table SI-1: Crystallographic data and structure refinement for (R)-(R,R) and (R)-(R,R)-benzene structures.

Identification code	(R)Binol-(R,R)DADPE **(R)-(R,R)**	(R)Binol-(R,R)DADPE **(R)-(R,R)-benzene**
CCDC Number	2295235	2295236
Empirical formula	C_{20} H_{14} O_2, C_{14} H_{16} N_2	C_{20} H_{14} O_2, C_{14} H_{16} N_2, 2.7(C_6 H_6)
Formula weight	498.60	710.46
Temperature	297(2) K	150(2) K
Wavelength	0.71073 Å	0.71073 Å
Crystal system	Tetragonal	Tetragonal
Space group	$P4_12_12$	$I422$
Unit cell dimensions	a = 13.32025(13) Å	a = 23.5398(17) Å
	b = 13.32025(13) Å	b = 23.5398(17) Å
	c = 31.8915(6) Å	c = 15.3506(9) Å
	α = 90°.	α = 90°.
	β = 90°.	β = 90°.
	γ = 90°.	γ = 90°.
Volume	5658.48(15) Å^3	8506.1(14) Å^3
Z	8	8
Density (calculated)	1.171 Mg/m^3	1.110 Mg/m^3
Absorption coefficient	0.073 mm^{-1}	0.067 mm^{-1}
F(000)	2112	3023
Crystal size	0.32 x 0.30 x 0.25 mm^3	0.50 x 0.04 x 0.04 mm^3
Theta range for data collection	3.125 to 26.616°.	2.915 to 18.849°.
Index ranges	-16<=h<=16, -16<=k<=16, -36<=l<=40	-21<=h<=21, -21<=k<=21, -13<=l<=13
Reflections collected	37467	11492
Independent reflections	5837 [R(int) = 0.0584]	1682 [R(int) = 0.0864]
Completeness to theta = 18.849°	99.2 %	99.3 %
Absorption correction	Semi-empirical from equivalents	Semi-empirical from equivalents
Max. and min. transmission	1.00000 and 0.95306	1.00000 and 0.28300

Refinement method	Full-matrix least-squares on F^2	Full-matrix least-squares on F^2
Data / restraints / parameters	5837 / 97 / 382	1682 / 408 / 280
Goodness-of-fit on F^2	1.089	1.248
Final R indices [I>2sigma(I)]	R1 = 0.0394, wR2 = 0.1066	R1 = 0.1165, wR2 = 0.2486
R indices (all data)	R1 = 0.0449, wR2 = 0.1101	R1 = 0.1477, wR2 = 0.2667
Absolute structure parameter	0.1(5)	0.8(10)
Extinction coefficient	n/a	n/a
Largest diff. peak and hole	0.121 and -0.116 e.Å^{-3}	0.237 and -0.226 e.Å^{-3}

CCDC 2295235 and 2295236 contain the supplementary crystallographic data for this paper. These data can be obtained free of charge from The Cambridge Crystallographic Data Centre via www.ccdc.cam.ac.uk/structures.

Figure SI-1: (a) Asymmetric unit of the (R)-(R,R) cocrystal, (b) expanded asymmetric unit to show full molecules (disorder omitted for clarity).

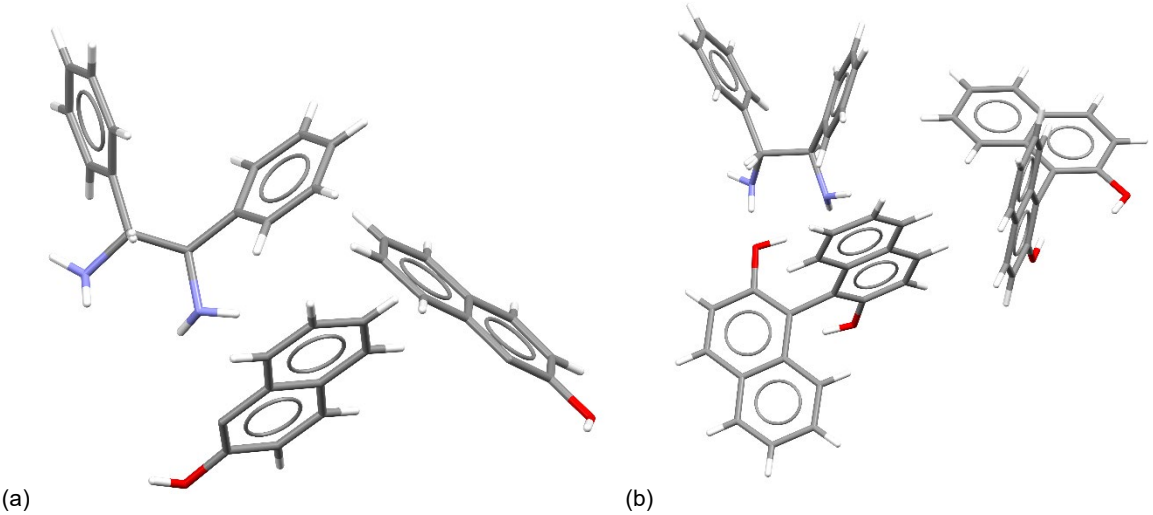

(a) (b)

Figure SI-2: (a) Asymmetric unit of the (R)-(R,R)-benzene cocrystal-solvate, (b) expanded asymmetric unit to show full molecules (disorder omitted for clarity).

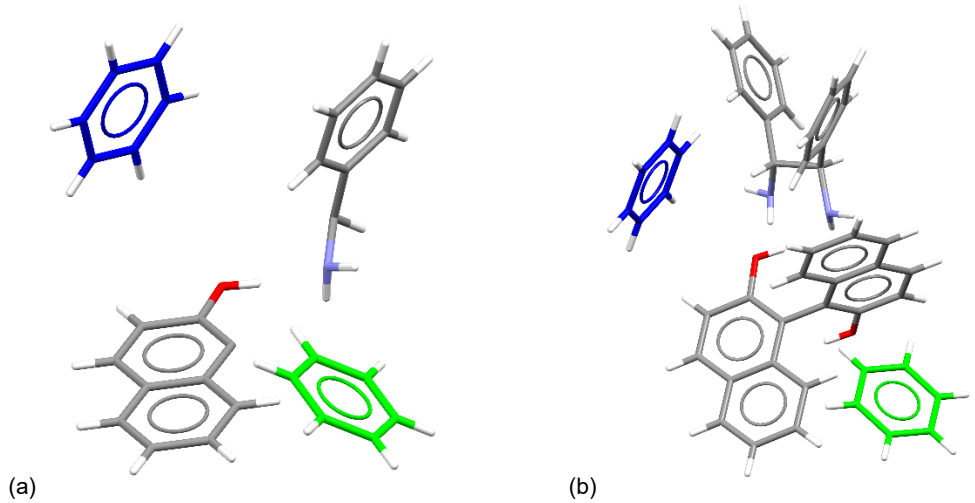

(a) (b)

2.2 Calculation of the void in (R)-(R,R)-benzene cocrystal-solvate structure

The volume of the voids, where no solvent molecules could be located, were calculated by Platon via Void/SOLV. The total potential solvent area volume = 583.7Å^3 (6.7% of the unit cell volume), distributed over two sites surrounding the 4-fold axes (284 Å^3, or about 3.33% of the unit cell).

2.3 Superposition of (R)-(R,R) solvated and non-solvated cocrystal structures.

Figure SI-3: (a) Superposition of the crystalline structures (R)-(R,R) (pink) and (R)-(R,R)-benzene (orange) structural motifs, showing a central common motif (composed of two Binol and two DADPE molecules). (b) Close-up of the overlaid molecules (disorder omitted for clarity).

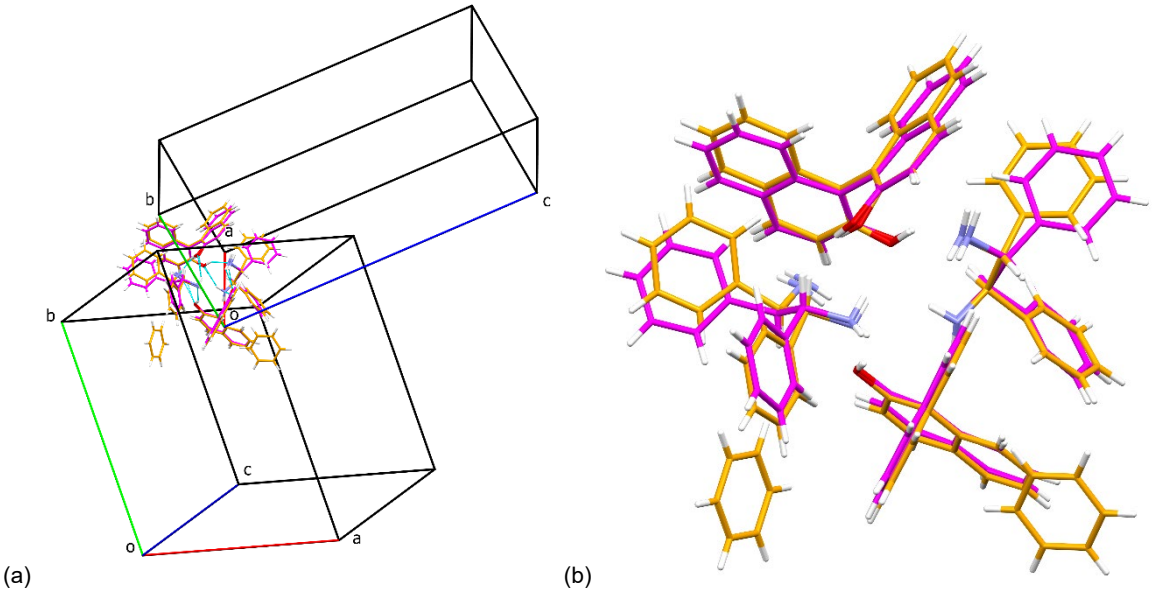

(a) (b)

3) Solvent screening experiment

3.1 Experimental data

Table SI-2: Experimental data for solvent screening for Binol:DADPE systems.

Reagent		Solvent	Binol :DADPE (mole ratio)	m (mg)		V solvent (mL)	P-XRD result
				Binol	DADPE		
(S)-Binol	(R,R)-DADPE	MeOH	1 :1	285.89	211.42	2	(S)-(R,R) cocrystal **DICVUH**
(S)-Binol	(R,R)-DADPE	EtOH	1 :1	186.02	211.12	2	(S)-(R,R) cocrystal **DICVUH**
(S)-Binol	(R,R)-DADPE	EtOAc	1:1	143.3	106.3	0.5	(S)-(R,R) cocrystal **DICVUH**
(S)-Binol	(R,R)-DADPE	DCM	1 :1	143.1	106.3	0.3	(S)-(R,R) cocrystal **DICVUH**
(S)-Binol	(R,R)-DADPE	toluene	1 :1	285.53	212.02	2	(S)-(R,R) cocrystal **DICVUH**
(S)-Binol	(R,R)-DADPE	IPA	1 :1	143.2	106.7	0.5	(S)-(R,R) cocrystal **DICVUH**
(S)-Binol	(R,R)-DADPE	benzene	1 :1	143.6	106.4	2	(S)-(R,R) cocrystal **DICVUH**
(R)-Binol	(R,R)-DADPE	MeOH	1 :1	286.91	212.44	0.5	(R)-(R,R) cocrystal CCDC: **2295235**

(R)-Binol	(R,R)-DADPE	EtOH	1 :1	286.29	211.9	2	(R)-(R,R) cocrystal CCDC: **2295235**
(R)-Binol	(R,R)-DADPE	EtOAc	1 :1	143.5	105.6	0.3	(R)-(R,R) cocrystal CCDC: **2295235**
(R)-Binol	(R,R)-DADPE	DCM	1 :1	143.6	106.9	0.2	(R)-(R,R) cocrystal CCDC: **2295235**
(R)-Binol	(R,R)-DADPE	toluene	1 :1	186.07	211.97	2	(R)-(R,R) cocrystal CCDC: **2295235**
(R)-Binol	(R,R)-DADPE	IPA	1 :1	143.2	105.1	0.5	(R)-(R,R) cocrystal CCDC: **2295235**
(R)-Binol	(R,R)-DADPE	benzene	1:1	143.5	105.9	2	(R)-(R,R)-benzene cocrystal-solvate CCDC: **2295236**

3.2 PXRD patterns

Figure SI-4: Comparison of the X-ray diffraction patterns (using Cu Kα) between 1:1 slurry outcomes of (S)-Binol and (R,R)-DADPE in MeOH (red), EtOH (brown), EtOAc (orange), DCM (light green), toluene (dark green), IPA (dark blue) and benzene (light blue) and the simulated pattern of the reported (S)-(R,R)-cocrystal **DICVUH**[1] (fuchsia).

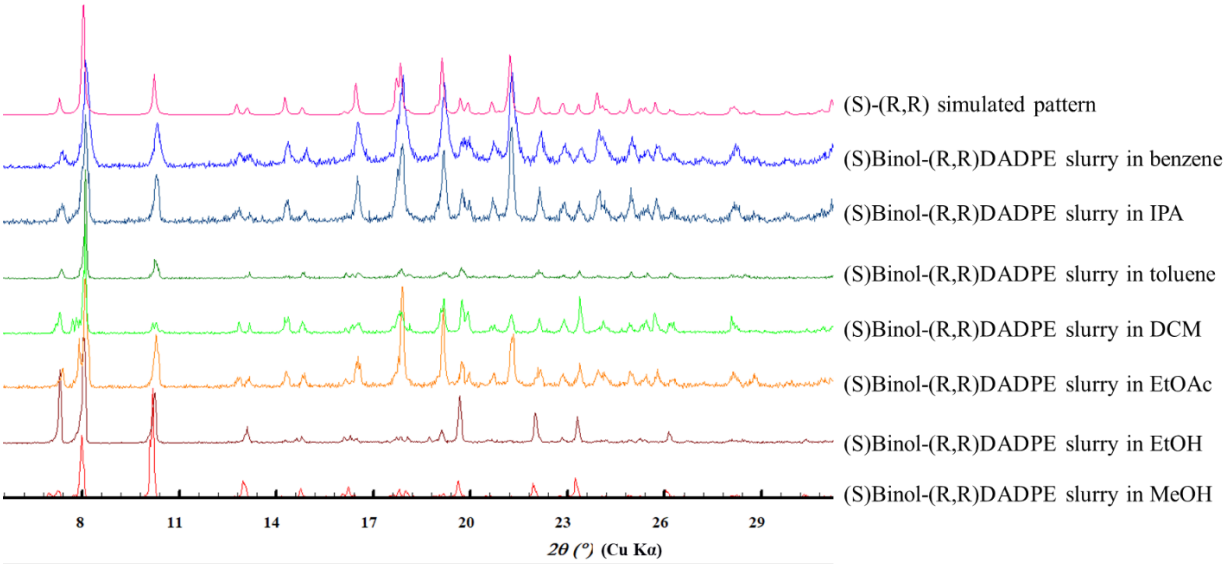

Figure SI-5: Comparison of the X-ray diffraction patterns (using Cu Kα) between the 1:1 slurry outcome of (R)-Binol and (R,R)-DADPE in MeOH (blue), EtOH (red), EtOAc (dark green), DCM (rose), toluene (brown) and IPA (in light green) and the simulated pattern of the (R)-(R,R)-cocrystal (black, current work – CCDC: **2295235**).

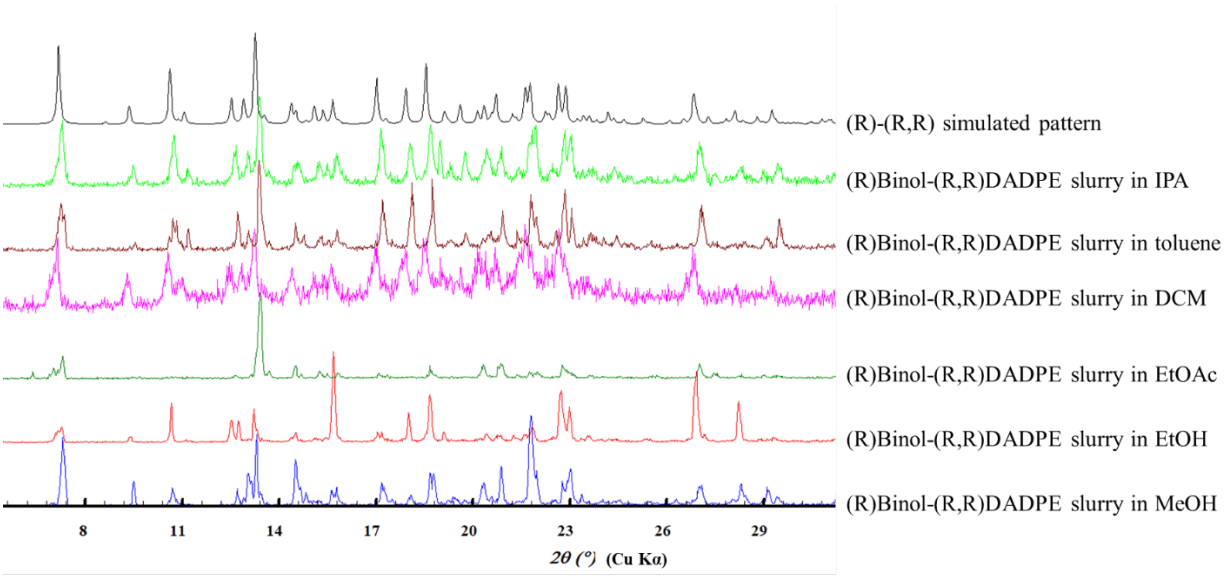

Figure SI-6: Comparison of the X-ray diffraction patterns (using Cu Kα) between the 1:1 slurry outcome of (R)-Binol and (R,R)-DADPE in benzene (blue) and the simulated pattern of the (R)-(R,R)-benzene cocrystal-solvate (in red, current work – CCDC: **2295236**).

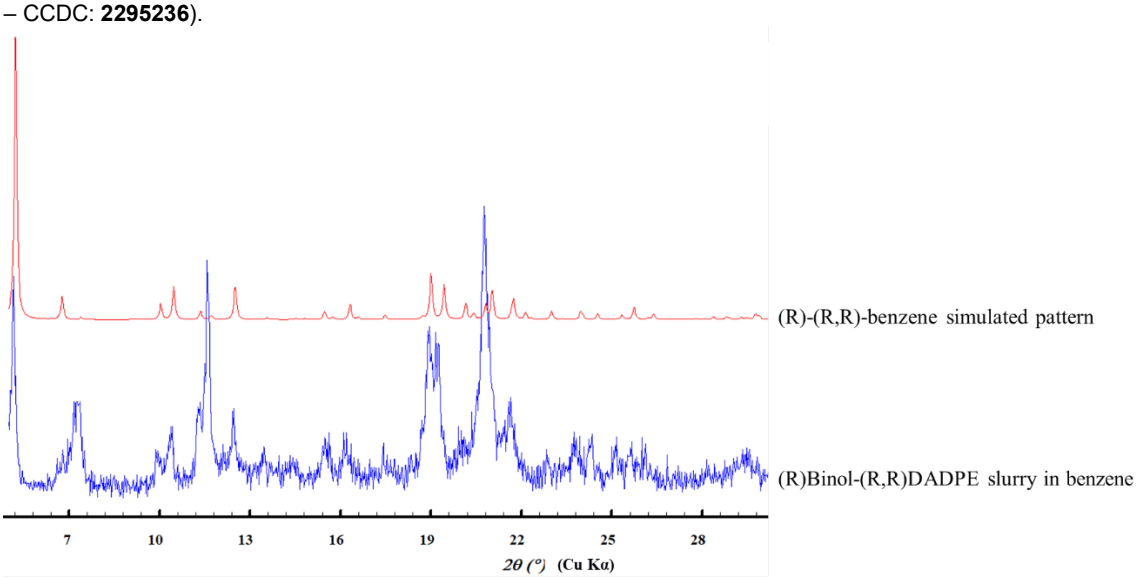

There are some intensity differences for low-angle peaks between simulated and experimental patterns. This can be explained by varying degree of pore filling.

4) Thermal analyses

4.1 Thermogravimetric analyses (TGA)

Figure SI-7: TGA of the (S)-(R,R) cocrystal, obtained slurrying a 1:1 ratio in toluene. The thermogram is expressed as the weight loss (%) with respect to temperature. The thermogram shows a single step mass loss starting at 141°C, consisting in the degradation of the product.

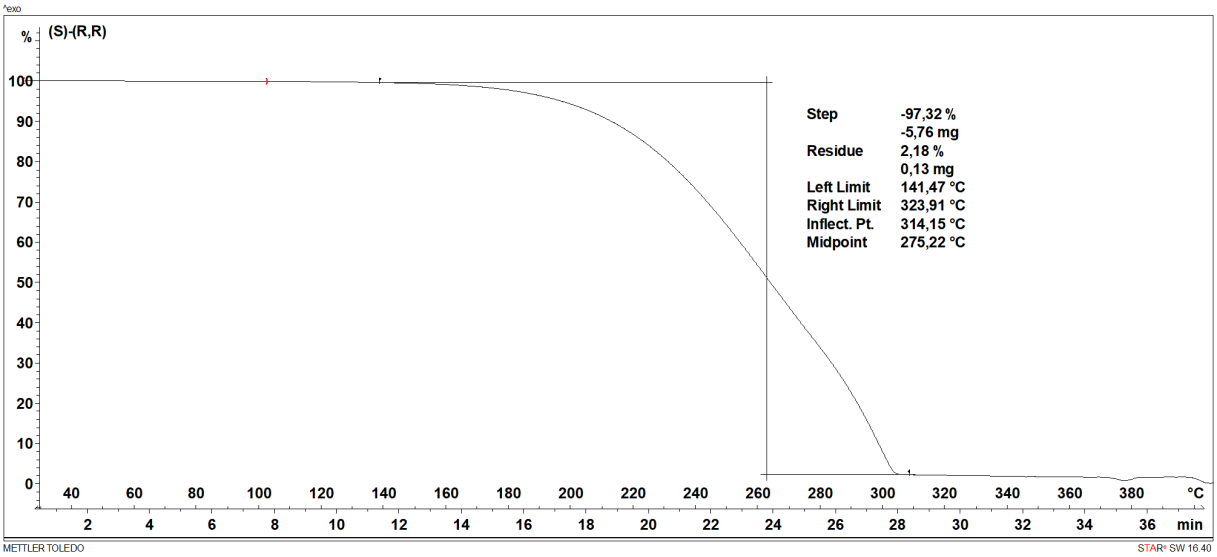

Figure SI-8: TGA of the (R)-(R,R) cocrystal, obtained slurrying a 1:1 ratio in toluene. The thermogram is expressed as the weight loss (%) with respect to temperature. The thermogram shows a single step mass loss starting at 143°C, consisting in the degradation of the product.

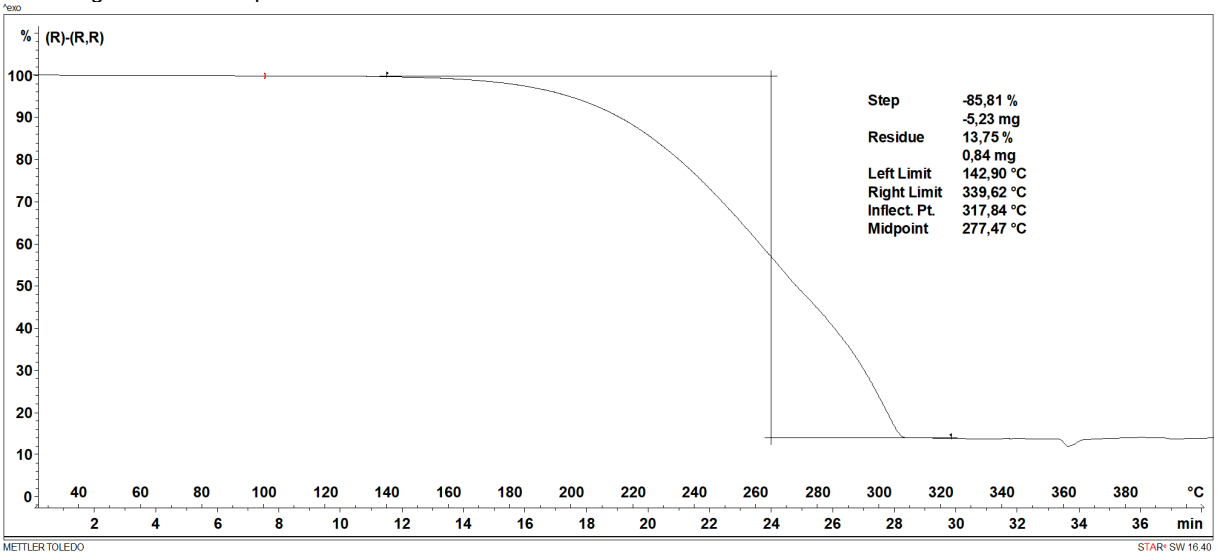

Figure SI-9: TGA of the (R)-(R,R)-benzene cocrystal-solvate, analyzed directly after filtration and obtained slurrying a 1:1 ratio in benzene. The thermogram is expressed as the weight loss (%) with respect to temperature. The thermogram shows multiple mass changes. The two first ones start at 19°C and consist in desolvation and evaporation of benzene inside the solvent channel (loss of 0.61 equivalent of benzene), the second mass change starts at 75°C and also represents desolvation (loss of 0.49 equivalent of benzene), the third mass change starts at 171°C and consists in the degradation of the compound.

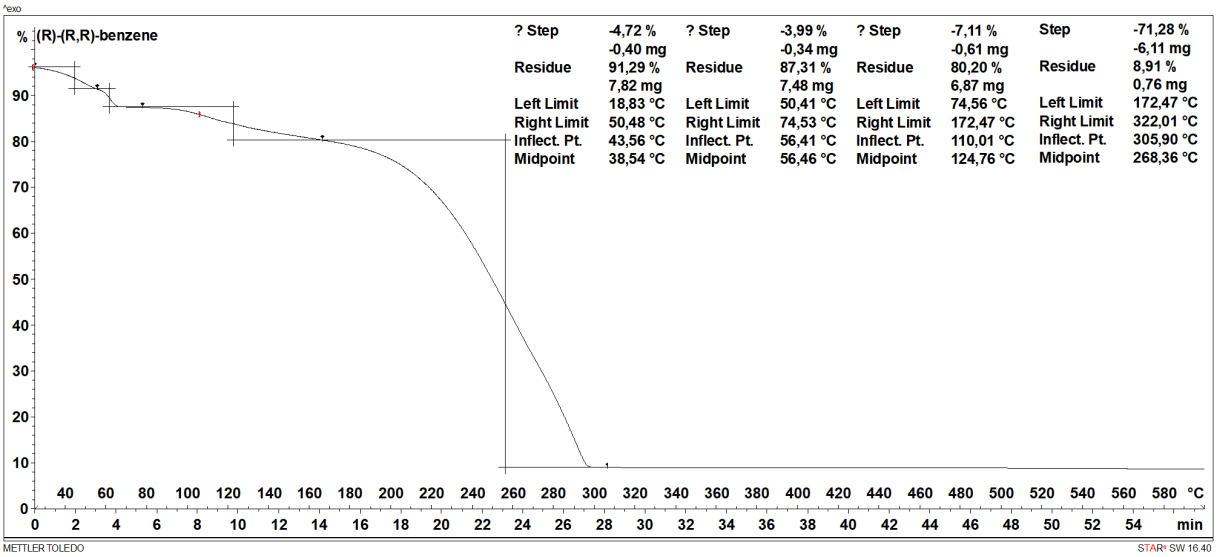

Figure SI-10: TGA of the (R)-(R,R)-benzene cocrystal-solvate, analyzed one week after filtration and obtained by slurry (1:1) in benzene. The thermogram is expressed as the weight loss (%) with respect to the increase of temperature.

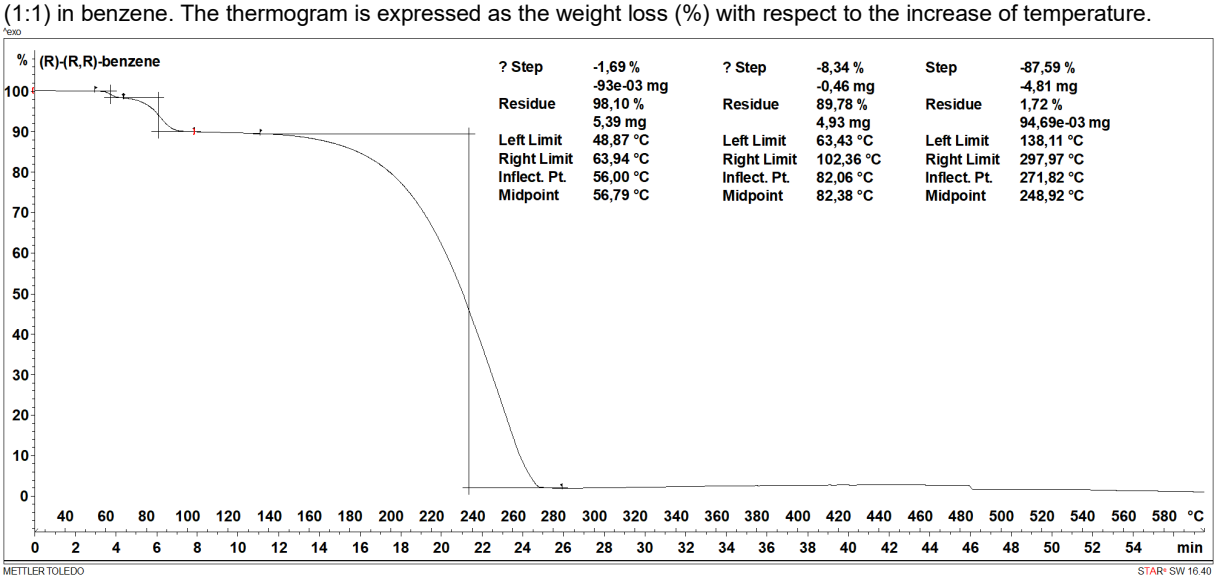

4.2 Differential scanning calorimetry analyses (DSC)

Figure SI-11: DSC of the (S)-(R,R) cocrystal, obtained slurrying a 1:1 ratio in toluene. The thermogram is expressed in mW with respect to the increase of temperature. The thermogram shows one endothermic peak, with onset at 128°C corresponding to the melt of the (S)-(R,R) cocrystal.

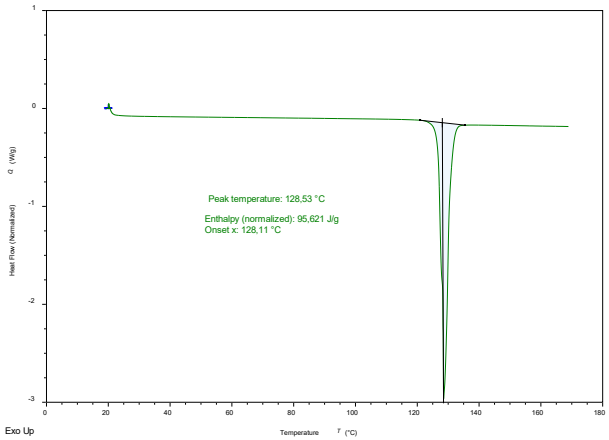

Figure SI-12: DSC of the (R)-(R,R) cocrystal, obtained slurrying a 1:1 ratio in toluene. The thermogram expressed in mW with respect to the increase of temperature. The thermogram shows one endothermic peak, with onset at 130°C corresponding to the melt of the (R)-(R,R) cocrystal.

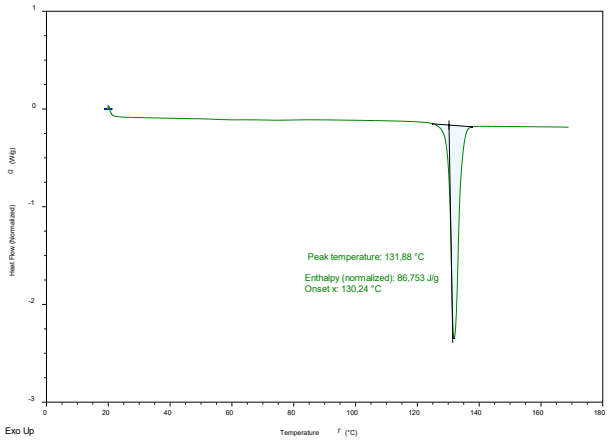

Figure SI-13: DSC of the (R)-(R,R)-benzene cocrystal-solvate, obtained slurrying a 1:1 mixture in benzene. The thermogram shows three different transitions. The two first endothermic peaks have an onset at respectively 50°C and 61°C, and consist in the desolvation of benzene from the different sites in the crystal and the third endothermic peak, which has an onset at 131°C, consists in the melt of the (R)-(R,R) cocrystal.

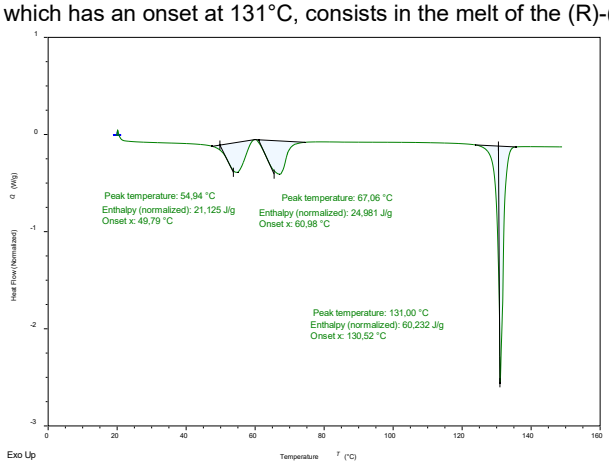

4.3 Variable temperature Powder X-ray diffraction analysis (VT-PXRD)

Figure SI-14: Variable temperature PXRD patterns (using Mo Kα) for the (R)-(R,R)-benzene cocrystal-solvate, obtained slurrying a 1:1 mixture in benzene and compared to the simulated patterns of the compounds (R)-(R,R)-benzene and (R)-(R,R) (black).

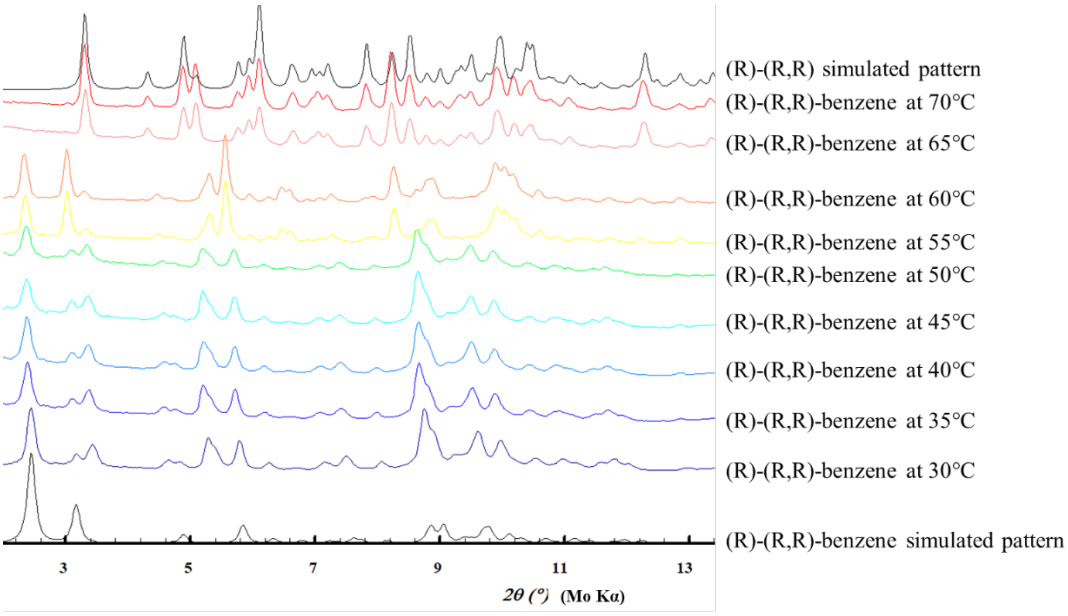

In Figures SI-15 to SI-17, Rietveld refinement was done to assign the majority phase for each temperature range. At both 30°C and 60°C, the (R)-(R,R)-benzene cocrystal-solvate exists as the dominant phase, at 65°C, the (R)-(R,R) cocrystal exists as the dominant phase.

Figure SI-15: Profile fitting of Rietveld refinement of the (R)-(R,R)-benzene cocrystal-solvate analyzed at 30°C.

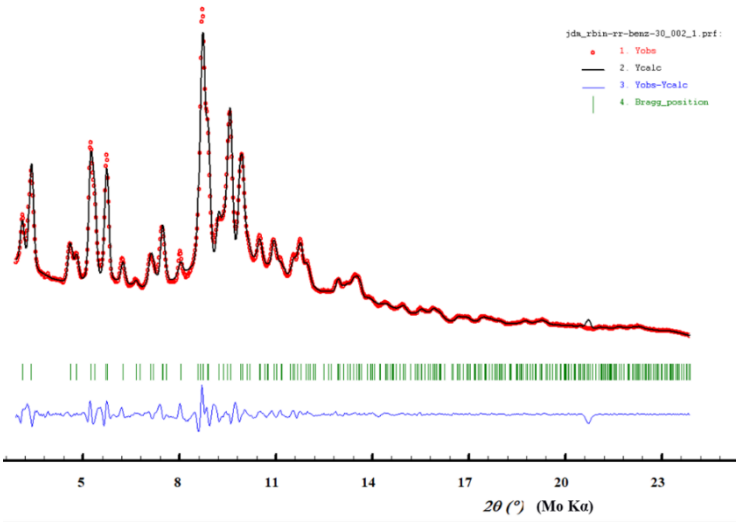

Figure SI-16: Profile fitting of Rietveld refinement of the (R)-(R,R)-benzene cocrystal-solvate analyzed at 60°C.

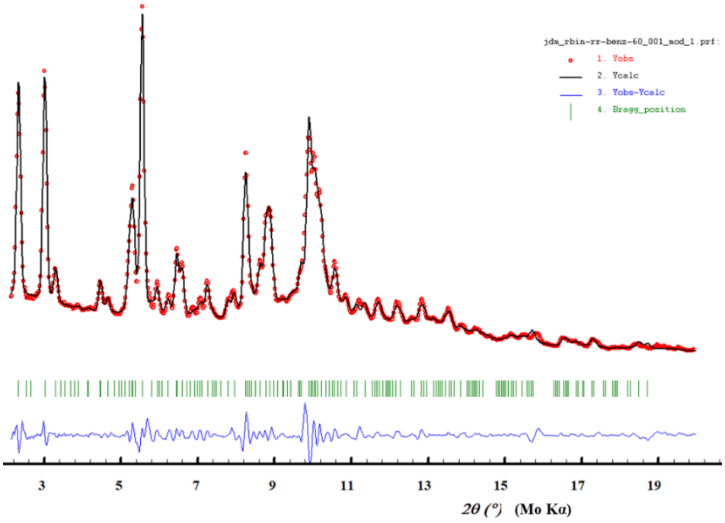

Figure SI-17: Profile fitting of Rietveld refinement of the (R)-(R,R) cocrystal analyzed at 65°C.

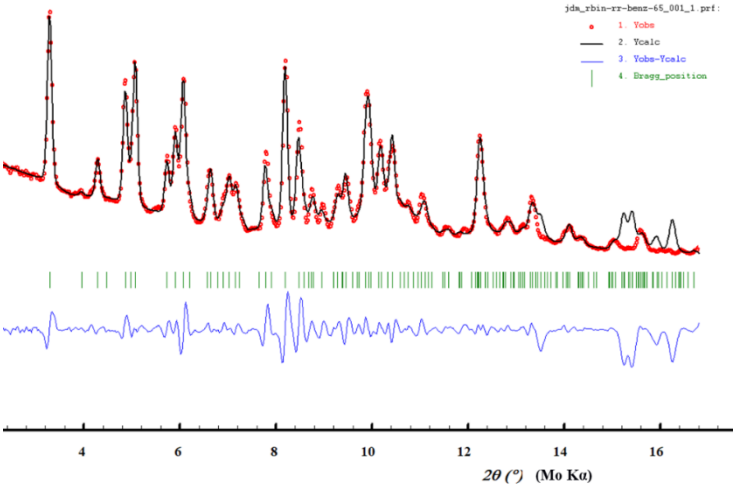

5) Solubility curves

5.1 In methanol (MeOH)

Table SI-3: Experimental data for the construction of the solubility curves of (R)-(R,R) and (S)-(R,R) cocrystals in MeOH.

m((S)-(R,R)) (g)	m(MeOH) (g)	C((S)-(R,R)) (g/mL)	T solub (°C)
0,14998	0,64564	0,1840	16,9
0,15567	0,63865	0,1930	18,8
0,14941	0,64575	0,1832	17,5
0,16501	0,63713	0,2051	21,7
0,16051	0,6515	0,1951	18,9
0,16517	0,64095	0,2041	21,1
0,17373	0,64927	0,2119	21,6
0,1697	0,64066	0,2098	22
0,17326	0,63935	0,2146	23,2
0,18217	0,64298	0,2244	23,8
0,18254	0,64803	0,2231	23,8
0,18268	0,64564	0,2241	24,3
0,19742	0,65766	0,2377	25,8

0,20031	0,64932	0,2443	26
0,20422	0,60241	0,2685	28,8
m((R)-(R,R)) (g)	m(MeOH) (g)	C((R)-(R,R)) (g/mL)	T solub (°C)
0,1496	0,64261	0,1844	18,1
0,14971	0,65269	0,1817	16,7
0,15055	0,64294	0,1855	16,8
0,15978	0,63944	0,1979	19,4
0,18061	0,64131	0,2230	24
0,17038	0,63975	0,2109	20
0,15956	0,647	0,1953	18,5
0,17066	0,63803	0,2118	20,1
0,15957	0,64004	0,1975	18,6
0,18043	0,64318	0,2222	21,9
0,2003	0,63467	0,2500	26,2
0,20036	0,64365	0,2465	26,9
0,20039	0,63356	0,2505	25,7
0,17029	0,64226	0,2100	21
0,17985	0,63964	0,2227	22,7

Figure SI-18: Solubility curves of (R)-(R,R) and (S)-(R,R) cocrystals in MeOH.

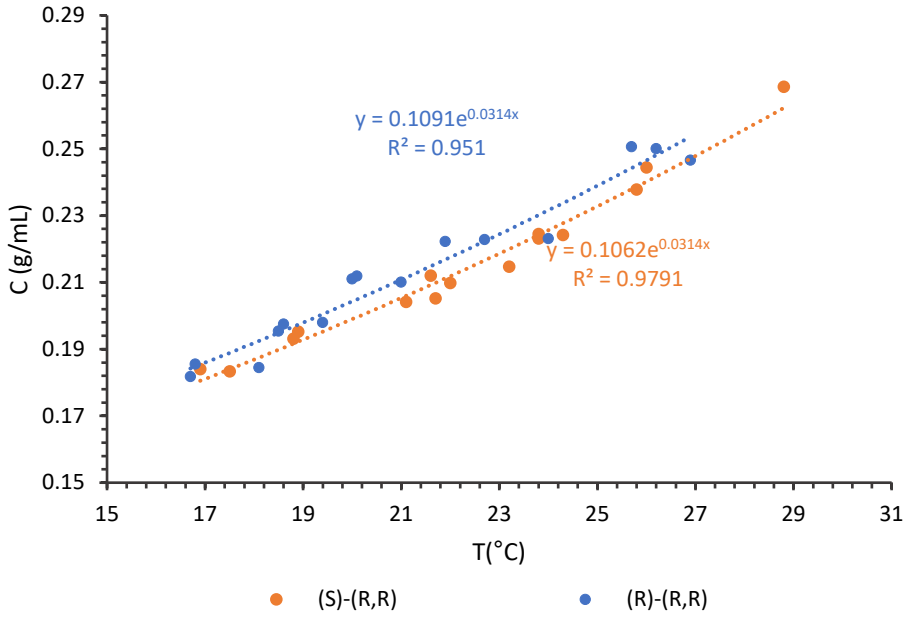

5.2 In ethanol (EtOH)

Table SI-4: Experimental data for the construction of the solubility curves of (R)-(R,R) and (S)-(R,R) cocrystals in EtOH.

m((R)-(R,R)) (g)	m(EtOH) (g)	C((R)-(R,R)) (g/mL)	T solub (°C)
0,07064	0,6269	0,0889	23,7
0,07976	0,60643	0,1038	28,5
0,0794	0,63338	0,0989	27,1
0,08088	0,63349	0,1007	28,2
0,09164	0,64836	0,1115	30,5
0,0917	0,64155	0,1128	31,1
0,10029	0,63129	0,1253	33,8
0,10207	0,64542	0,1248	34,3
0,11958	0,66151	0,1426	38,4

m((S)-(R,R)) (g)	m(EtOH) (g)	C((S)-(R,R)) (g/mL)	T solub (°C)
0,06991	0,64905	0,0850	26,1
0,07123	0,63756	0,0881	27,7
0,06997	0,63852	0,0865	27,2
0,07933	0,64424	0,0972	29,4
0,08074	0,64962	0,0981	31,1
0,08228	0,65059	0,0998	31,5
0,08955	0,65181	0,1084	33,3
0,08972	0,64648	0,1095	34,3
0,09031	0,64127	0,1111	34,3
0,10207	0,64659	0,1246	36,4
0,10014	0,65271	0,1210	36,1
0,10195	0,64847	0,1240	37,7
0,12232	0,64394	0,1499	41,4
0,12225	0,64085	0,1505	41,7
0,11957	0,64137	0,1471	41,4

Figure SI-19: Solubility curves of (R)-(R,R) and (S)-(R,R) cocrystals in EtOH.

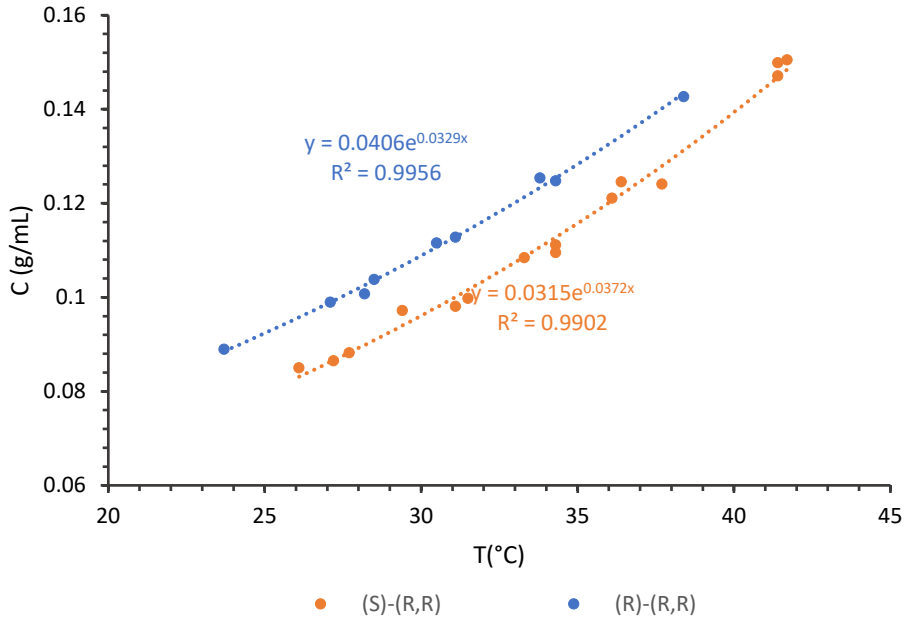

5.3 In isopropyl alcohol (IPA)

Table SI-5: Experimental data for the construction of the solubility curves of (R)-(R,R) and (S)-(R,R) cocrystals in IPA.

m((R)-(R,R)) (g)	m(EtOH) (g)	C((R)-(R,R)) (g/mL)	T solub (°C)
0,12917	0,61435	0,1653	54,7
0,1292	0,60698	0,1673	56,9
0,12921	0,61553	0,1650	56,6
0,04914	0,61816	0,0625	32
0,09832	0,6119	0,1263	47,7
0,09835	0,6159	0,1255	43,1
0,06866	0,6225	0,0867	32
0,06868	0,61803	0,0873	39,4
0,01826	0,62388	0,0230	16
0,01833	0,62486	0,0231	11,7
0,01827	0,61564	0,0233	13,2

m((S)-(R,R)) (g)	m(IPA) (g)	C((S)-(R,R)) (g/mL)	T solub (°C)
0,13033	0,61144	0,1675	62,6
0,13024	0,60917	0,1680	62,8
0,13034	0,61842	0,1657	62,6
0,09931	0,61526	0,1269	57,8
0,09925	0,62002	0,1258	59
0,09923	0,61112	0,1276	59,2
0,04876	0,62099	0,0617	48,7
0,0488	0,61731	0,0621	49,4
0,04882	0,60292	0,0636	50
0,02074	0,6104	0,0267	31,4
0,02078	0,61673	0,0265	27,2
0,02073	0,6186	0,0263	32,1

Figure SI-20: Solubility curves of (R)-(R,R) and (S)-(R,R) cocrystals in IPA.

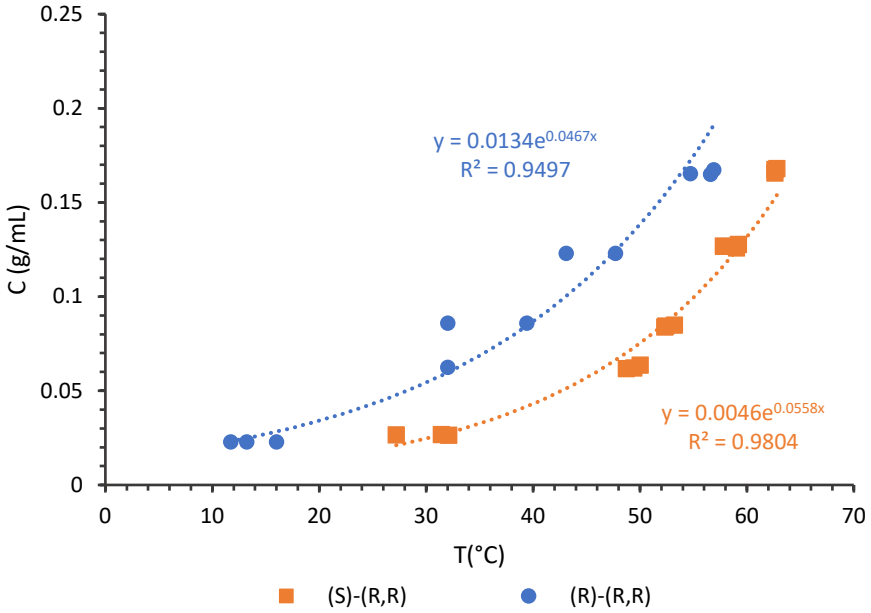

5.4 In toluene

Table SI-6: Experimental data for the construction of the solubility curves of (R)-(R,R) and (S)-(R,R) cocrystals in toluene.

m((R)-(R,R)) (g)	m(EtOH) (g)	C((R)-(R,R)) (g/mL)	T solub (°C)
0,05031	0,70854	0,0616	27,5
0,06944	0,70018	0,0860	31,6
0,07194	0,69934	0,0892	32,4
0,06966	0,70822	0,0853	31,8
0,08147	0,70309	0,1005	35,3
0,07927	0,71615	0,0960	34,6
0,07973	0,6961	0,0993	36,4
0,09974	0,70524	0,1226	40,8
0,09955	0,69375	0,1244	41,2
0,10046	0,71079	0,1225	40,8
m((S)-(R,R)) (g)	m(tolu) (g)	C((S)-(R,R)) (g/mL)	T solub (°C)
0,05072	0,70977	0,0620	43,9
0,05037	0,71068	0,0614	43,9
0,05103	0,70682	0,0626	44,8

0,06035	0,71097	0,0736	46,5
0,07059	0,70935	0,0863	46,1
0,08061	0,70278	0,0994	47,3
0,08255	0,69548	0,1029	48,1
0,08032	0,70418	0,0989	47,5
0,09977	0,71797	0,1205	50,5
0,10116	0,70318	0,1247	51,1
0,10156	0,70455	0,1250	51,5

Figure SI-21: Solubility curves of (R)-(R,R) and (S)-(R,R) cocrystals in toluene.

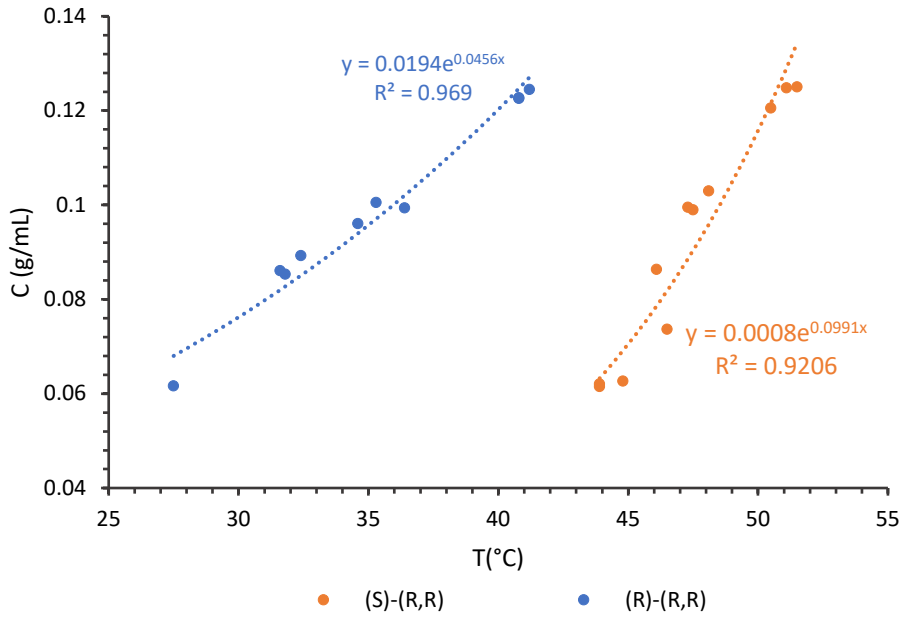

5.5 In benzene

Table SI-7: Experimental data for the construction of the solubility curves of (R)-(R,R)-benzene and (S)-(R,R) cocrystals in benzene.

m((S)-(R,R)) (g)	m(benzene) (g)	C((S)-(R,R)) (g/mL)	T solub (°C)
0,0442	0,9414	0,0411	20,4
0,0507	0,8663	0,0513	23,9
0,0566	0,9257	0,0536	25,4
0,0221	0,9737	0,0199	8,1
0,0273	1,0695	0,0224	8,1
0,03516	0,70284	0,0438	21,8
0,03466	0,70449	0,0431	21,6
0,03554	0,70424	0,0442	22,1
0,05192	0,70538	0,0645	28,6
0,04514	0,69737	0,0567	26,6
m((R)-(R,R)) (mg)	m(benzene) (g)	C((R)-(R,R)-benzene) (g/mL)	T solub (°C)
10,13	617,5	0,0144	15,5
15,13	631,01	0,0210	20,8
20,31	623,98	0,0285	25,1
25,22	627,73	0,0352	28,1

30,21	621,04	0,0426	31,1
35,26	623,03	0,0496	33,4
40,08	628,36	0,0559	35,2
45,06	628,83	0,0628	36,4
10,13	956,6	0,0093	10,7
15,13	965,44	0,0137	17,1
20,31	972,53	0,0183	21
25,22	975,95	0,0226	24,3
35,2600	971,75	0,0318	28,7
40,0800	966,35	0,0363	31,1
45,0600	961,71	0,0410	32,5

Figure SI-22: Solubility curves of (S)-(R,R) cocrystal and (R)-(R,R)-benzene cocrystal-solvate in benzene.

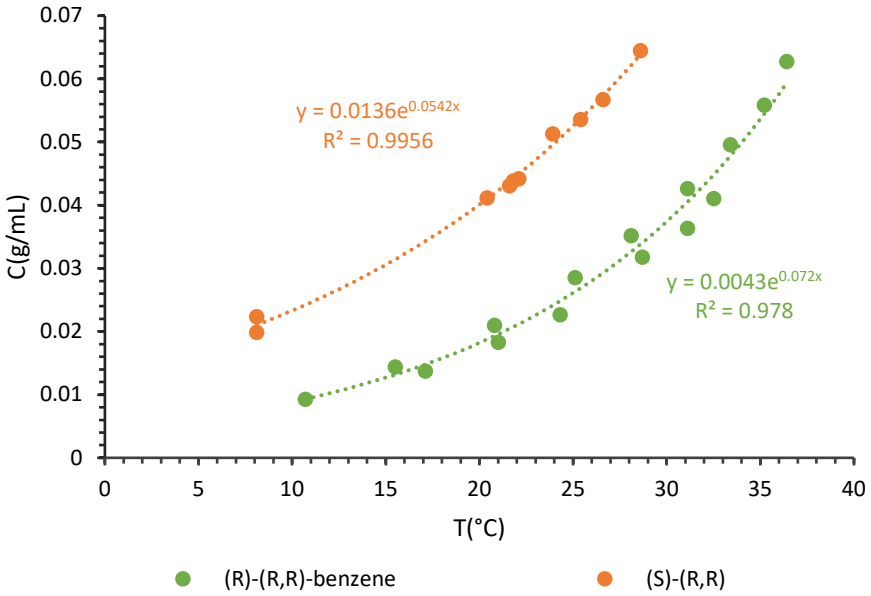

6) Isoplethal ternary diagram experiments and results

6.1 In toluene

Table SI-8: Experimental data and results for the construction of the isoplethal ternary diagram (rac)-Binol-(R,R)DADPE-toluene at 20°C.

		m(tolu) (mg)	m((rac)-Binol) (mg)	m((R,R)-DADPE) (mg)	%mol(tolu)	%mol((rac)-Binol)	%mol((R,R)-DADPE)	PXRD results	ratio Binol:DADPE determined by NMR	ratio (S)-:(R)-Binol determined by cHPLC	point
98,50%	1	1717,1	70,95	8,21	0,9849	0,0131	0,0020	(rac)-Binol	X	x	(rac)-Binol
	2	1731,46	60,31	16,4	0,9849	0,0110	0,0040	(rac)-Binol	1 :0	x	(rac)-Binol
	3	1722,97	49,3	24,14	0,9849	0,0091	0,0060	(rac)-Binol	1 :0	x	(rac)-Binol
	4	1716,91	38,33	32,49	0,9848	0,0071	0,0081				soluble
	5	1715,15	27,27	40,42	0,9849	0,0050	0,0101				soluble
	6	1711,84	16,39	48,57	0,9848	0,0030	0,0121				soluble
	7	1723,78	5,61	56,64	0,9849	0,0010	0,0140				soluble
97%	1	1724,57	144,61	16,48	0,9698	0,0262	0,0040	(rac)-Binol	x	x	(rac)-Binol
	2	1713,34	127,69	28,88	0,9697	0,0233	0,0071	(rac)-Binol	x	x	(rac)-Binol
	3	1716,8	111,44	41,26	0,9696	0,0203	0,0101	(rac)-Binol (+ (S)-(R,R)*)	1 :0,07	x	(rac)-Binol
	4	1736,57	88,83	57,53	0,9701	0,0160	0,0139	(rac)-Binol + (S)-(R,R)	x	x	(rac)-Binol + (S)-(R,R)
	5	1729,85	72,22	69,91	0,9700	0,0130	0,0170	(S)-(R,R)	x	99,88 :0,12	(S)-(R,R)
	6	1723,47	55,47	82,36	0,9698	0,0100	0,0201	(S)-(R,R)	x	100 :0	(S)-(R,R)
	7	1727,03	33,41	98,65	0,9699	0,0060	0,0240				soluble
	8	1714,13	16,71	111,23	0,9696	0,0030	0,0273				soluble
	9	1724,54	0	123,21	0,9699	0,0000	0,0301	(R,R)-DADPE	x	x	(R,R)-DADPE
96%	1	1714,98	196,17	20,29	0,9597	0,0353	0,0049	(rac)-Binol	x	x	(rac)-Binol
	2	1732,36	168,22	41,76	0,9600	0,0300	0,0100	(rac)-Binol	x	x	(rac)-Binol
	3	1733,87	140,37	62,3	0,9600	0,0250	0,0150	(rac)-Binol + (S)-(R,R)	x	x	(rac)-Binol + (S)-(R,R)
	4	1727,3	112,25	83,33	0,9598	0,0201	0,0201	(rac)-Binol + (S)-(R,R)	1 :0,825	x	(rac)-Binol + (S)-(R,R)
	5	1730,98	84,24	103,99	0,9599	0,0150	0,0250	(S)-(R,R)	x	x	(S)-(R,R)
	6	1734,49	56,14	124,98	0,9600	0,0100	0,0300	(S)-(R,R)	0,7 :1	x	(S)-(R,R) + (R,R)-DADPE
	7	1723,8	28,12	145,46	0,9598	0,0050	0,0352	(R,R)-DADPE	0 :1	x	(R,R)-DADPE
95%	1	1723,65	249,56	25,13	0,9497	0,0443	0,0060	(rac)-Binol	x	x	(rac)-Binol
	2	1724,2	215,56	50,49	0,9497	0,0382	0,0121	(rac)-Binol + (S)-(R,R)	1 :0,07	x	(rac)-Binol

	3	1726,41	181,59	75,46	0,9498	0,0322	0,0180	(rac)-Binol + (S)-(R,R)	x	x	(rac)-Binol + (S)-(R,R)
	4	1718,07	147,34	100,59	0,9497	0,0262	0,0241	(rac)-Binol + (S)-(R,R) (+(R)-(R,R)*)	x	x	(rac)-Binol + (S)-(R,R) +(R)-(R,R)
	5	1715,05	113,5	126,16	0,9495	0,0202	0,0303	(S)-(R,R)	x	99,45 :0,55	(S)-(R,R)
	6	1733,37	79,28	151,55	0,9500	0,0140	0,0360	(S)-(R,R) (+ (R,R)DADPE*)	0,89 :1	x	(S)-(R,R) + (R,R)-DADPE
	7	1722,18	45,41	176,23	0,9498	0,0081	0,0422	(R,R)-DADPE	0,145 :1	x	(S)-(R,R) + (R,R)-DADPE
	8	1738,44	11,48	201,77	0,9501	0,0020	0,0479	(R,R)-DADPE	0 :1	x	(R,R)-DADPE
93%	1	1717,84	347,67	42,51	0,9295	0,0605	0,0100	(rac)-Binol	1 :0	x	(rac)-Binol
	2	1720,35	289,79	85,37	0,9296	0,0504	0,0200	(rac)-Binol + (S)-(R,R)	x	x	(rac)-Binol + (S)-(R,R)
	3	1726,58	231,53	128,57	0,9298	0,0401	0,0301	(rac)-Binol + (S)-(R,R) (+ (R)-(R,R)*)	x	x	(rac)-Binol + (S)-(R,R) + (R)-(R,R)
	4	1717,1	173,42	171,22	0,9296	0,0302	0,0402	(rac)-Binol + (S)-(R,R) (+ (R)-(R,R)*)	x	x	(rac)-Binol + (S)-(R,R) + (R)-(R,R)
	5	1723,23	115,64	214,74	0,9296	0,0201	0,0503	(S)-(R,R)	x	98,47 :1,53	(S)-(R,R)
	6	1717,6	57,96	257,52	0,9294	0,0101	0,0605	(R,R)-DADPE	0,13 :1	x	(S)-(R,R) + (R,R)-DADPE
90%	1	1715,58	538,8	44,29	0,8991	0,0909	0,0101	(rac)-Binol	1 :0	x	(rac)-Binol
	2	1719,6	478,34	88,22	0,8995	0,0805	0,0200	(rac)-Binol + (S)-(R,R)	x	x	(rac)-Binol + (S)-(R,R)
	3	1726,56	419,01	133,33	0,8996	0,0703	0,0302	(rac)-Binol + (S)-(R,R) + (R)-(R,R)	x	x	(rac)-Binol + (S)-(R,R) + (R)-(R,R)
	4	1728,44	359,81	177,37	0,8997	0,0603	0,0401	(rac)-Binol + (S)-(R,R) + (R)-(R,R)	x	x	(rac)-Binol + (S)-(R,R) + (R)-(R,R)
	5	1730,31	299,47	222,05	0,8998	0,0501	0,0501	(S)-(R,R) + (R)-(R,R) (+ (rac)-Binol*)	x	x	(rac)-Binol + (S)-(R,R) + (R)-(R,R)
	6	1725,61	239,32	266,25	0,8996	0,0401	0,0602	(S)-(R,R) + (R)-(R,R)	0,965 :1	x	(S)-(R,R) + (R)-(R,R)
	7	1714,44	179,88	310,86	0,8989	0,0304	0,0707	(S)-(R,R)	x	x	(S)-(R,R)
	8	1724,2	119,72	355,52	0,8994	0,0201	0,0805	(S)-(R,R) (+ (R,R)-DADPE*)	0.6 :1	x	(S)-(R,R) + (R,R)-DADPE
	9	1729,85	59,61	399,53	0,8998	0,0100	0,0902	(R,R)-DADPE	0,05 :1	x	(R,R)-DADPE

* only trace amounts are visible

-The three points 95% - 4, 93% - 3 and - 4 (in yellow) were difficult to interpret due to trace amounts. The (R)-(R,R) cocrystal seemed to present in trace amounts in these samples.

6.2 In benzene

Table SI-9: Experimental data and results for the construction of the isoplethal ternary diagram (rac)-Binol-(R,R)-DADPE-benzene at 20°.

		m(benz) (mg)	m((rac)-Binol) (mg)	m((R,R)-DADPE) (mg)	%mol(benz)	%mol((rac)-Binol)	%mol((R,R)-DADPE)	PXRD results	ratio Binol:DADPE determined by NMR	ratio (S)-/(R)-Binol determined by cHPLC	point
98,50%	4	1736,01	58,75	28,96	0,9849	0,0091	0,0060	(rac)-Binol (+ (R)-(R,R)-benzene?)	1:0,16	x	(rac)-Binol + (R)-(R,R)-benzene
	5	1745,41	45,63	38,4	0,9850	0,0070	0,0080	(R)-(R,R)-benzene (+(rac)-Binol*)	1:0,925	4,34:95,66	(rac)-Binol + (R)-(R,R)-benzene
	6	1748,77	32,6	48,44	0,9850	0,0050	0,0100				soluble
	7	1737,38	19,52	58,42	0,9848	0,0030	0,0122				soluble
	8	1745,46	6,6	67,64	0,9849	0,0010	0,0140				soluble
	9	1750	0	72,5	0,9850	0,0000	0,0150	(R,R)-DADPE	X	x	(R,R)-DADPE
97%	3	1746,43	152,26	34,2	0,9699	0,0231	0,0070	(rac)-Binol	1:0	x	(rac)-Binol
	4	1743,17	132,36	48,98	0,9699	0,0201	0,0100	(rac)-Binol (+ (R)-(R,R)-benzene*)	1:0,245	x	(rac)-Binol + (R)-(R,R)-benzene
	5	1747,61	105,86	68,79	0,9699	0,0160	0,0140	(R)-(R,R)-benzene	X	0,68:99,32	(R)-(R,R)-benzene
	6	1741,96	86,06	83,31	0,9699	0,0131	0,0171	(R)-(R,R)-benzene	X	0,50:99,50	(R)-(R,R)-benzene
	7	1739	66,35	98,04	0,9698	0,0101	0,0201	(R)-(R,R)-benzene	X	0:100	(R)-(R,R)-benzene
	8	1751,62	39,72	117,72	0,9700	0,0060	0,0240	(R)-(R,R)-benzene + (R,R)-DADPE	0,155:1	x	(R)-(R,R)-benzene + (R,R)-DADPE
	9	1750,56	19,54	132,28	0,9701	0,0030	0,0270	(R,R)-DADPE	X	x	(R,R)-DADPE
96%	2	1745,59	234,12	24,61	0,9599	0,0351	0,0050	(rac)-Binol	X	x	(rac)-Binol
	3	1743,14	200,35	49,53	0,9599	0,0301	0,0100	(rac)-Binol	1:0,1	x	(rac)-Binol + (R)-(R,R)-benzene
	4	1737,81	167,25	74,37	0,9597	0,0252	0,0151	(rac)-Binol + (R)-(R,R)-benzene	x	x	(rac)-Binol + (R)-(R,R)-benzene
	5	1747,43	133,56	99,24	0,9599	0,0200	0,0201	(R)-(R,R)-benzene + (S)-(R,R)	1:0,965	x	(R)-(R,R)-benzene + (S)-(R,R)
	6	1748,07	100,28	123,88	0,9599	0,0150	0,0250	(R)-(R,R)-benzene	x	1,28:98,72	(R)-(R,R)-benzene
	7	1752,37	66,69	148,67	0,9601	0,0100	0,0300	(R)-(R,R)-benzene	1:0.99	0:100	(R)-(R,R)-benzene
	8	1743,7	33,54	173,01	0,9599	0,0050	0,0350	(R,R)-DADPE (+ (R)-(R,R)-benzene*)	(0,087:1)	x	(R,R)-DADPE
95%	2	1747,39	297,24	30,23	0,9499	0,0441	0,0060	(rac)-Binol	1:0	x	(rac)-Binol
	3	1748,72	256,59	60,24	0,9499	0,0380	0,0120	(rac)-Binol (+ (R)-(R,R)-benzene*)	1:0,17	x	(rac)-Binol + (R)-(R,R)-benzene
	4	1740,16	216,37	90,24	0,9497	0,0322	0,0181	(rac)-Binol + (R)-(R,R)-benzene	x	x	(rac)-Binol + (R)-(R,R)-benzene

	5	1740,08	175,55	120,2	0,9497	0,0261	0,0241	(R)-(R,R)-benzene + (S)-(R,R)	1:0,915	x	(R)-(R,R)-benzene + (S)-(R,R)
	6	1741,35	135,3	150,15	0,9497	0,0201	0,0301	(R)-(R,R)-benzene + (S)-(R,R)	x	x	(R)-(R,R)-benzene + (S)-(R,R)
	7	1746,18	94,63	180,48	0,9498	0,0140	0,0361	(R)-(R,R)-benzene	x	0,57:99,43	(R)-(R,R)-benzene
	8	1744,11	54,39	210,21	0,9498	0,0081	0,0421	(R,R)-DADPE (+(R)-(R,R)-benzene*)	0,19:1	x	(R)-(R,R)-benzene + (R,R)-DADPE
	9	1745,38	13,25	240,42	0,9499	0,0020	0,0481	(R,R)-DADPE	x	x	(R,R)-DADPE
93%	1	1752,68	414,36	51,59	0,9300	0,0600	0,0101	(rac)-Binol	1:0,03	x	(rac)-Binol
	2	1733,71	345,77	102,7	0,9292	0,0506	0,0203	(rac)-Binol + (R)-(R,R)-benzene	x	x	(rac)-Binol + (R)-(R,R)-benzene
	3	1742,16	276,32	153,23	0,9297	0,0402	0,0301	(rac)-Binol + (R)-(R,R)-benzene + (S)-(R,R)	1:0,675	x	(rac)-Binol + (R)-(R,R)-benzene + (S)-(R,R)
	4	1737,74	207,1	204,28	0,9296	0,0302	0,0402	(R)-(R,R)-benzene + (S)-(R,R)	1:0,925	x	(R)-(R,R)-benzene + (S)-(R,R)
	5	1744,6	138,09	256,14	0,9297	0,0201	0,0502	(R)-(R,R)-benzene	x	6,31:93,69	(R)-(R,R)-benzene + (S)-(R,R)
	6	1752,39	69,14	307,63	0,9299	0,0100	0,0601	(R)-(R,R)-benzene + (R,R)-DADPE	0,158:1	x	(R)-(R,R)-benzene + (R,R)-DADPE
90%	1	1745,13	642,19	52,26	0,8998	0,0903	0,0099	(rac)-Binol	1:0,025		(rac)-Binol
	2	1752,06	570,29	105,86	0,9001	0,0799	0,0200	(rac)-Binol + (R)-(R,R)-benzene	1:0,165	x	(rac)-Binol + (R)-(R,R)-benzene
	3	1742,57	499,48	158,75	0,8995	0,0703	0,0302	(rac)-Binol + (R)-(R,R)-benzene (+ (S)-(R,R)*)	1:0,425	x	(rac)-Binol + (R)-(R,R)-benzene + (S)-(R,R)
	4	1750,66	428,38	211,46	0,8999	0,0601	0,0400	(rac)-Binol + (R)-(R,R)-benzene + (S)-(R,R)	x	x	(rac)-Binol + (R)-(R,R)-benzene + (S)-(R,R)
	5	1745,47	356,92	264,55	0,8996	0,0502	0,0502	(R)-(R,R)-benzene + (S)-(R,R) (+(rac)-Binol*)	1:1.025	x	(R)-(R,R)-benzene + (S)-(R,R)
	6	1740,69	285,79	317,12	0,8994	0,0403	0,0603	(R)-(R,R)-benzene + (S)-(R,R)	x	x	(R)-(R,R)-benzene + (S)-(R,R)
	7	1751,41	214,52	370,45	0,8999	0,0301	0,0700	(R)-(R,R)-benzene + (S)-(R,R)	x	x	(R)-(R,R)-benzene + (S)-(R,R)
	8	1644,68	143,03	423,16	0,8941	0,0212	0,0846	(R)-(R,R)-benzene (+(S)-(R,R)*)	x	3,73:96,27	(R)-(R,R)-benzene + (S)-(R,R)
	9	1744,68	71,22	476,49	0,8996	0,0100	0,0904	(R,R)-DADPE (+ (R)-(R,R)-benzene*)	0,12:1	x	(R)-(R,R)-benzene + (R,R)-DADPE

* only trace amounts are visible

7) Resolution of Binol with (S,S)-DADPE

Figure SI-23: *c*HPLC analysis of the powder recovered from the resolution of (rac)-Binol by (S,S)-DADPE in benzene.

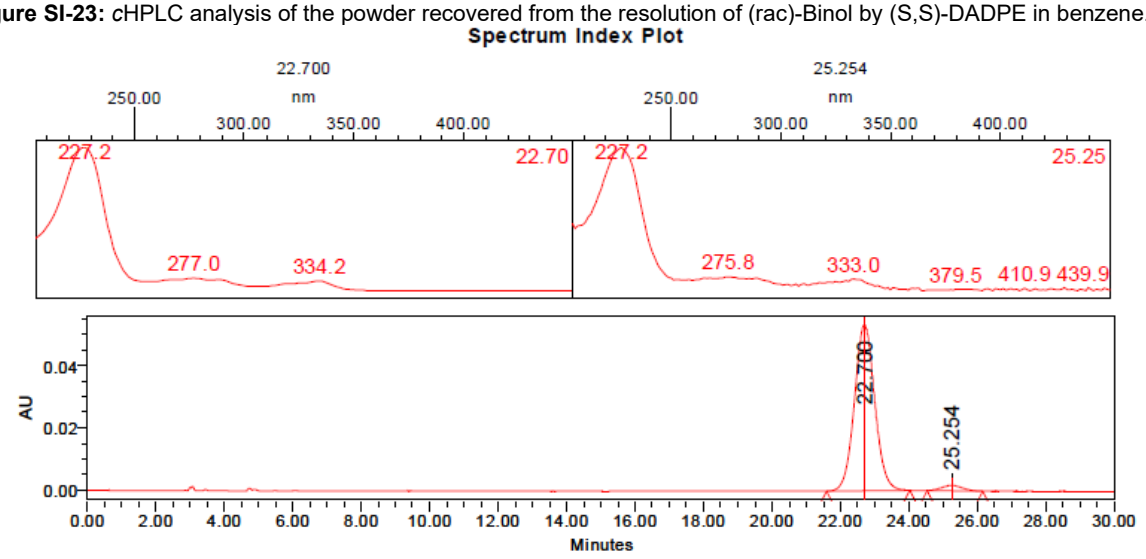

Peak Results

	Name	RT	Area	% Area
1		22.700	2178080	96.77
2		25.254	72587	3.23

8) Upscaled resolutions of Binol

8.1 In toluene

Figure SI-24: PXRD (using Cu Kα) of the powder recovered from the resolution of 2g of (rac)-Binol by (R,R)-DADPE in toluene, compared to the simulated pattern of the (S)-(R,R) cocrystal (**DICVUH**[1]).

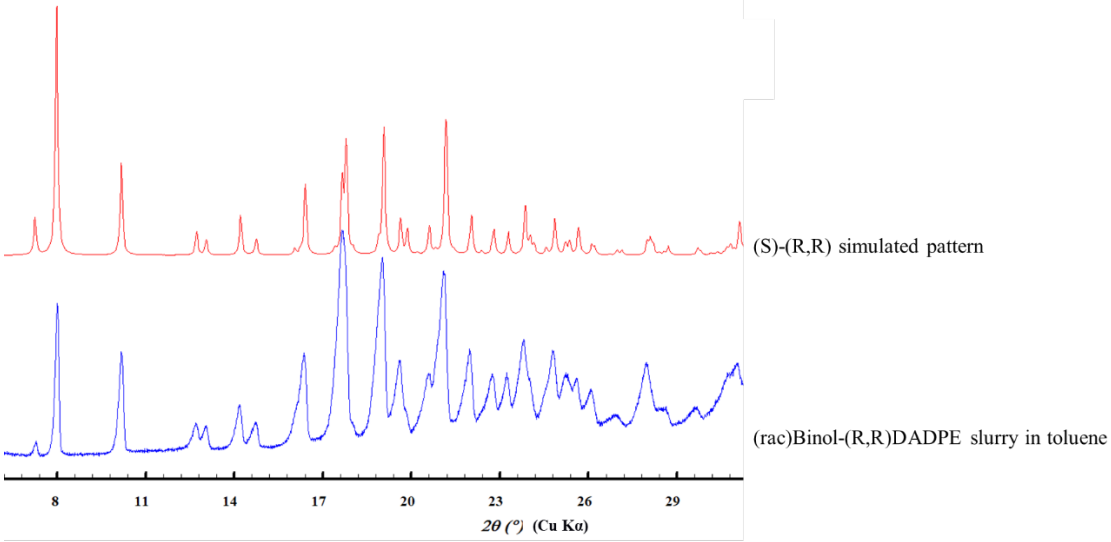

Figure SI-25: *c*HPLC analysis of the powder recovered from the resolution of 2g of (rac)-Binol by (R,R)-DADPE in toluene.

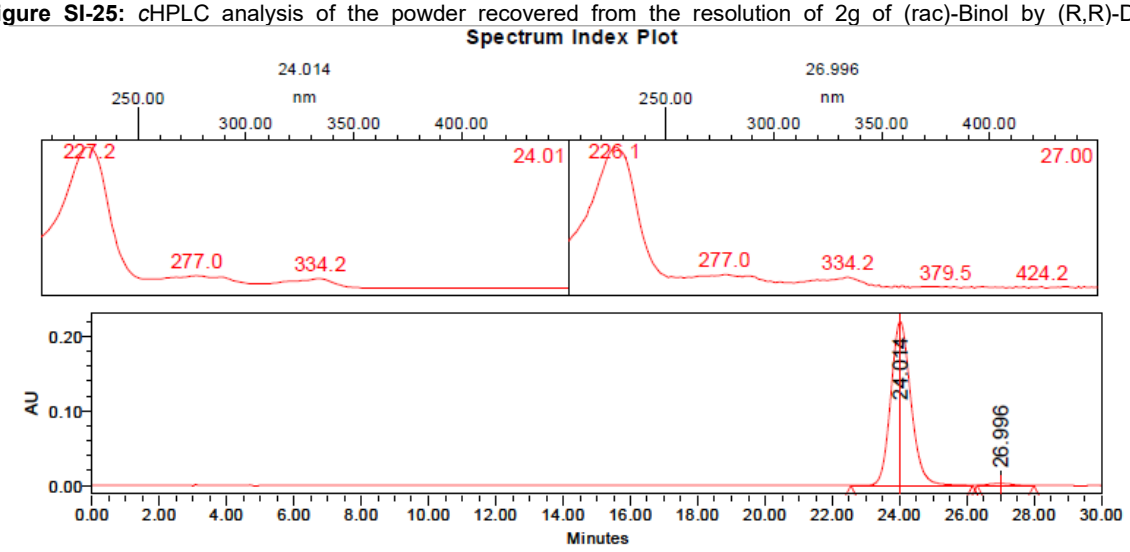

Peak Results

	Name	RT	Area	% Area
1		24.014	9143007	98.78
2		26.996	112873	1.22

8.2 In benzene

Figure SI-26: PXRD (using Cu Kα) of the powder recovered from the resolution of 2g of (rac)-Binol by (R,R)-DADPE in benzene, compared to the measured and the simulated patterns of the (R)-(R,R)-benzene cocrystal-solvate.

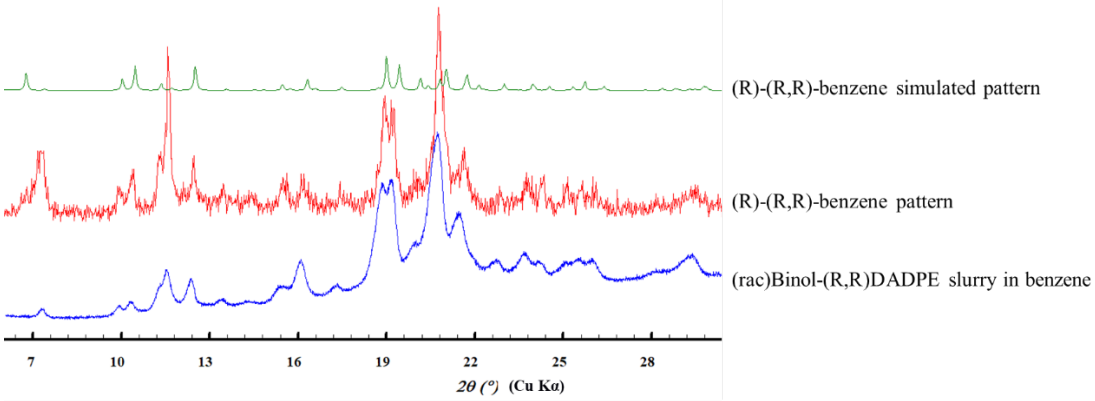

Figure SI-27: *c*HPLC analysis of the powder recovered from the resolution of 2g of (rac)-Binol by (R,R)-DADPE in benzene.

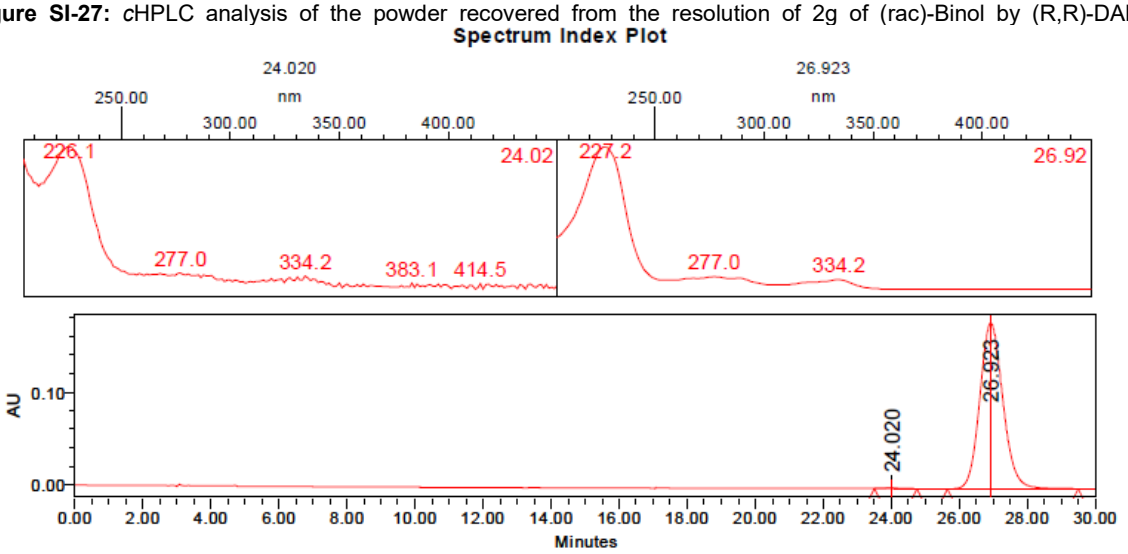

Peak Results

	Name	RT	Area	% Area
1		24.020	29781	0.35
2		26.923	8392381	99.65

References

1 M. Ratajczak-Sitarz, A. Katrusiak, K. Gawrońska, J. Gawroński, *Tetrahedron: Asymmetry,* **2007**, *18* (6), 765–773.

2 CrysAlisPro, Version 1.171.37.35; Rigaku Oxford Diffraction.

3 G. M. Sheldrick, *Acta Crystallogr., Sect. A: Found. Adv.*, **2015**, *71*, 3-8.

4 G. M. Sheldrick, *Acta Crystallogr., Sect. C: Struct. Chem.*, **2015**, *71*, 3–8.

5 A. L. Spek, *Acta Crystallogr., Sect. D: Biol. Crystallogr.*, **2009**, *65*, 148–155.

6 C. F. Macrae, I. Sovago, S. J. Cottrell, P. T. A. Galek, P. McCabe, E. Pidcock, M. Platings, G. P. Shields, J. S. Stevens, M. Towler and P. A. Wood, *J. Appl. Cryst*. **2020**, *53* (1), 226-235.

7 A. L. Spek, *Acta Crystallogr., Sect. C: Struct. Chem.*, **2015**, *71*, 9–18.